



## High $\beta$ produced by neutral beam injection in the START (Small Tight Aspect Ratio Tokamak) spherical tokamak

Alan Sykes

Citation: [Phys. Plasmas](#) **4**, 1665 (1997); doi: 10.1063/1.872271

View online: <http://dx.doi.org/10.1063/1.872271>

View Table of Contents: <http://pop.aip.org/resource/1/PHPAEN/v4/i5>

Published by the [American Institute of Physics](#).

---

### Related Articles

The effects of neutral gas heating on H mode transition and maintenance currents in a 13.56MHz planar coil inductively coupled plasma reactor  
[Phys. Plasmas](#) **19**, 093501 (2012)

Collisionless inter-species energy transfer and turbulent heating in drift wave turbulence  
[Phys. Plasmas](#) **19**, 082309 (2012)

Development of a low-energy and high-current pulsed neutral beam injector with a washer-gun plasma source for high-beta plasma experiments  
[Rev. Sci. Instrum.](#) **83**, 083504 (2012)

A stochastic mechanism of electron heating  
[Phys. Plasmas](#) **19**, 082506 (2012)

Toroidal ripple transport of beam ions in the mega-ampère spherical tokamak  
[Phys. Plasmas](#) **19**, 072514 (2012)

---

### Additional information on Phys. Plasmas

Journal Homepage: <http://pop.aip.org/>

Journal Information: [http://pop.aip.org/about/about\\_the\\_journal](http://pop.aip.org/about/about_the_journal)

Top downloads: [http://pop.aip.org/features/most\\_downloaded](http://pop.aip.org/features/most_downloaded)

Information for Authors: <http://pop.aip.org/authors>

## ADVERTISEMENT

The advertisement features the 'AIP Advances' logo at the top, which includes a series of orange circles of varying sizes. Below the logo, the text 'Special Topic Section: PHYSICS OF CANCER' is displayed in a bold, white font against a dark green background. Underneath this, the phrase 'Why cancer? Why physics?' is written in a lighter green font. A blue button with the text 'View Articles Now' is positioned at the bottom right of the advertisement. The background of the entire advertisement is a green and white abstract pattern of curved lines.

AIP Advances

Special Topic Section:  
**PHYSICS OF CANCER**

Why cancer? Why physics? [View Articles Now](#)

# High $\beta$ produced by neutral beam injection in the START (Small Tight Aspect Ratio Tokamak) spherical tokamak\*

Alan Sykes<sup>†</sup>

UKAEA Fusion (UKAEA/Euratom Fusion Association), Culham, Abingdon, Oxon OX14 3DB,  
United Kingdom

(Received 12 November 1996; accepted 20 January 1997)

The world's first high-power auxiliary heating experiments in a tight aspect ratio (or spherical) tokamak have been performed on the Small Tight Aspect Ratio Tokamak (START) device [Sykes *et al.*, Nucl. Fusion **32**, 694 (1992)] at Culham Laboratory, using the 40 keV, 0.5 MW Neutral Beam Injector loaned by the Oak Ridge National Laboratory. Injection has been mainly of hydrogen into hydrogen or deuterium target plasmas, with a one-day campaign to explore D→D operation. In each case injection provides a combination of higher density operation and effective heating of both ions and electrons. The highest  $\beta$  values achieved to date in START are volume average  $\beta_T \sim 11.5\%$  and central beta  $\beta_O \sim 50\%$ . Already high, these values are expected to increase further with the use of higher beam power. © 1997 American Institute of Physics. [S1070-664X(97)93305-X]

## I. INTRODUCTION

The economic feasibility of a fusion power plant requires stable operation at high values of beta, typically 5%–10%, where  $\beta = 2\mu_0 \langle p \rangle / B^2$  is the ratio of the volume averaged plasma pressure to the pressure of the magnetic field  $B$ .

The Troyon beta limit<sup>1</sup> implies that high values of beta should be achievable at low aspect ratio, indeed this is one of the perceived attractions of the Spherical Tokamak (ST). This can be seen by expressing the original form of the Troyon limit

$$\beta_T = \beta_N I_p a B_0 \text{ using } q_{\text{cyl}} = 5_2^q \kappa B_0 / R I_p,$$

in the form

$$\beta_T = \beta_N 5 \kappa / A q_{\text{cyl}}, \quad (1)$$

where we use the ‘‘experimentalists’’ definition of volume averaged beta  $\beta_T = (2\mu_0 / V B_0^2) \int p \, dV$ , and  $I_p$  (MA) is the plasma current,  $a$  (m) and  $R$  (m) the plasma minor and major radii,  $A = R/a$  the aspect ratio,  $\kappa$  the elongation, and  $B_0(T)$  the vacuum toroidal magnetic field at the geometric center of the discharge. Use of the value  $\beta_N = 4$  in (1) recovers the expression derived by considerations of ballooning mode stability in Sykes *et al.*<sup>2</sup>

The ST combines high natural elongation  $\kappa$  with low aspect ratio  $A$ . Typical plasmas in START (the Small Tight Aspect Ratio Tokamak) for example have aspect ratio  $A = 1.3$  with elongation  $\kappa$  from 1.5 to 2, and stability (at low beta) has previously been demonstrated experimentally at safety factors down to  $q_{\text{cyl}} \sim 1$ . Expression (1) therefore implies very high values of  $\beta_T$  may be attainable, if sufficient plasma heating can be obtained and if, as predicted computationally,<sup>3</sup> the Troyon expression remains valid at low  $A$ .

Key features of the START device and of the 40 keV neutral beam injector loaned by Oak Ridge National Laboro-

tory (ORNL) are described in Sec. II. The main results of the injection experiments to date are summarized in Sec. III, which gives details of the ion and electron heating obtained, and Sec. IV where high values of volume average  $\beta$  (11.5%) and central  $\beta$  (50%) are reported. It is found that the maximum beta values obtained appear to be limited by the beam power available and by low- $q$  operational limits. Magneto-hydrodynamic (MHD) behavior during injection is described in Sec. V. Differences in the properties between double null divertor (DND) and naturally limited plasmas are discussed in Sec. VI and VII, and plans for further neutral beam injection (NBI) experiments on START are outlined in Sec. VIII.

## II. MAIN FEATURES OF START AND THE ORNL INJECTOR

Although originally a low-budget experiment based on spare equipment,<sup>4</sup> START has been continuously upgraded and present operation features plasmas of up to  $R = 0.34$  m,  $a = 0.27$  m, plasma currents of over 250 kA and a plasma duration of longer than 40 ms.<sup>5</sup> The operating space is at least as large as for conventional tokamaks, and the energy confinement time is as good as or better than high-confinement mode (H-mode) scalings from conventional devices.<sup>6</sup> An important experimental feature is that an internal relaxation event, from which the plasma recovers, replaces the major disruption seen in conventional tokamaks. The present START configuration is shown in Fig. 1.

In 1994, it was decided to augment the program by testing the effects of additional heating by neutral beam injection and a 40 keV neutral beam injector was lent to Culham by ORNL for this purpose. To support this program, the START plasma diagnostics have recently been much improved, with the addition of a 30-point Thomson scattering system, a high-speed video camera capable of 40 000 frames/second, three new soft x-ray (SXR) cameras, 20-channel spectroscopic ion temperature diagnostics and a 16-channel neutral particle analyzer (NPA) capable of observing energies up to 50 keV.<sup>7</sup>

Operation of the ORNL beam began at Culham in late 1995 with tangential coinjection into START plasmas (mod-

\*Paper FIB4, Bull. Am. Phys. Soc. **41**, 1559 (1996).

<sup>†</sup>Invited speaker.

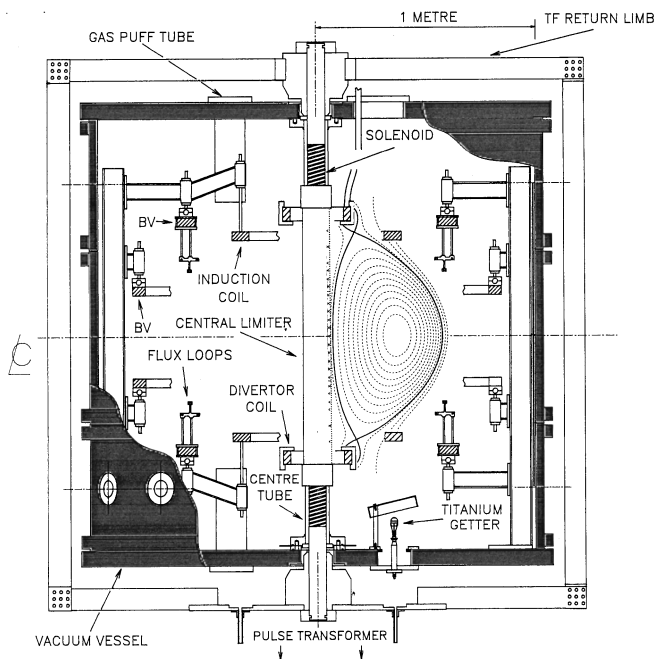


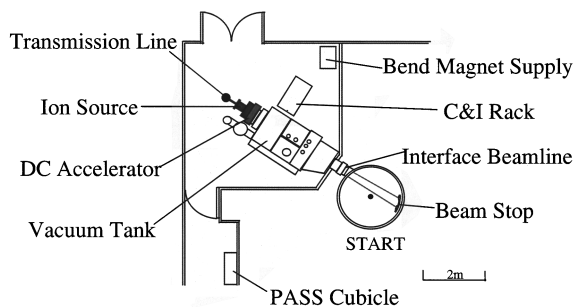
FIG. 1. Layout of the START experiment, October 1996.

eling and experiment have shown<sup>8</sup> that heating is poor using counterinjection). Since then the beam and plasma parameters have been steadily optimized and improved.

An outline diagram of the beam geometry in the START experiment is shown in Fig. 2. It is set up to inject power tangentially in the co-direction and has an impact parameter of  $R=0.28$  m. The beam has a divergence of  $1.3^\circ$  and is focused to achieve a  $1/e$  half-width of 12–13 cm in the plasma. Estimates using calorimetry suggest that the injected neutral beam power is up to  $400 \pm 100$  kW at an ion current of 54 A at 29 keV in hydrogen. The ion current reaches its flat-top in approximately 4 ms. A visible spectrometer was used to show that the  $H^+ : H_2^+ : H_3^+ : H_2O^+$  ion current ratio was 0.73:0.18:0.07:0.02. In deuterium operation at 41 A, 30 keV the species ratio was 0.79:0.12:0.08:0.01.

### III. NBI HEATING IN START

Injection of hydrogen neutrals into a hydrogen plasma began at low power levels in December 1995. More recently



START Neutral Beam Injection Geometry

FIG. 2. The ORNL neutral beam injector on START.

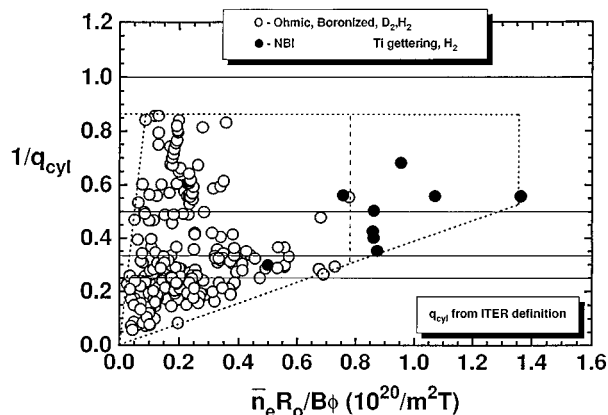


FIG. 3. Hugill diagram for START. Ohmic discharges—open symbols, NBI discharges—solid symbols.

deuterium target plasmas have been used, giving improved performance, and a one-day campaign injecting deuterium into a deuterium plasma has been undertaken. In all cases during injection, the plasma exhibits heating of both ions and electrons, and higher Murakami parameter  $\tilde{n}_c R/B$  is achieved, as shown in Fig. 3.

Results of a typical NBI heating experiment, START #30868, are shown in Figs. 4 and 5. In this case, about 400 kW of hydrogen neutrals is injected into a hydrogen target plasma. Plasma current and line integral density traces are shown in Figs. 4(a) and 4(b). The total plasma energy (thermal and fast ion) is determined by equilibrium reconstruction, fitting to  $B_v$  coils on the center column, flux loops (shown in Fig. 1), the diamagnetic flux signal, and the position of the magnetic axis indicated from SXR analysis.

The total plasma energy,  $\beta_T$ , and  $\beta_N$  are shown as a function of time in Figs. 5(b)–5(d). It is seen that the energy

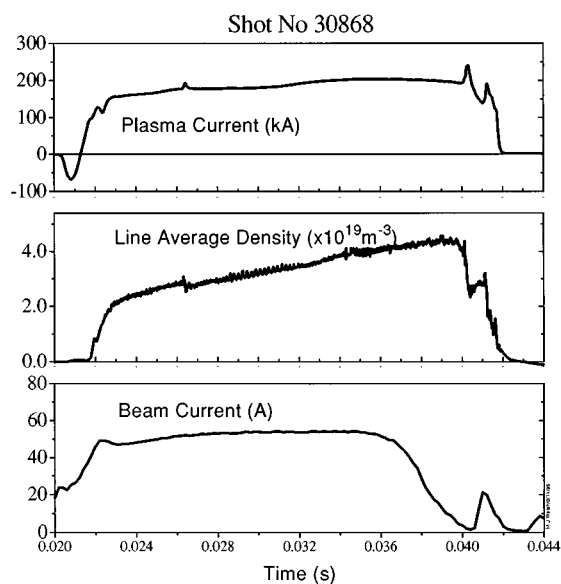


FIG. 4. Experimental traces of plasma current, line integral density, and beam current for START #30868. The negative current at the start is a feature of the induction process.

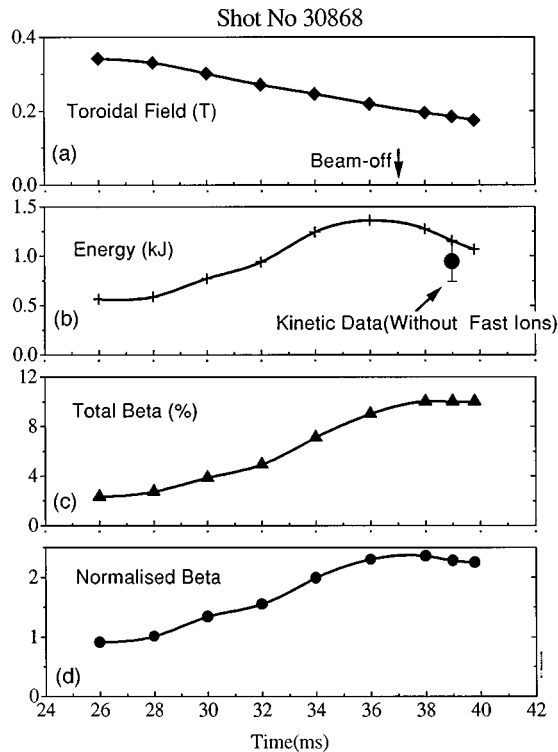


FIG. 5. For the same shot as Fig. 4: (a) Toroidal field at the geometric center; (b) total plasma energy obtained by equilibrium code reconstruction. A kinetic measurement is shown at  $t=39$  ms. (c) Total beta and (d)  $\beta_N$  vs time.

increases from 560 J, which is typical of Ohmic discharges, to a maximum of  $\sim 1200$  J at time 36 ms. At time 39 ms the electron temperature and density profile is measured by the 30-point Thomson scattering diagnostic and at this time the energy is derived kinetically, including thermal ion energy estimated from the ion temperature measured along chords by charge-exchange spectroscopy. When the beam is on, the fast ion component of plasma energy is estimated by Fokker-Planck modeling to be 200–300 J. However, at time 36 ms in this discharge the beam power reduces over 2–3 ms [Fig. 4(c)] and the slowing down time is  $\sim 2$  ms, so that at time 39 ms the fast ion component is estimated to be small ( $\sim 100$  J, i.e., about 10%). The kinetic estimate of the total plasma energy (but omitting the fast ion component) is indicated in Fig. 5(b), and is seen to be in good agreement with the magnetic reconstruction.

During this discharge the toroidal field is slowly reduced to increase beta. Figures 5(c) and 5(d) trace the evolution of total and normalized beta, which attain values of  $\beta_T \sim 10\%$  and  $\beta_N \sim 2.4$ , and which are held for times longer than an energy confinement time (about 2 ms).

Initially, the plasma current profile is broad but becomes more peaked in time with NBI heating. As the profile evolves  $m=2$  activity is seen on SXR cameras and on the interferometer  $\int ndl$  midplane trace, Fig. 4(b). At  $t \sim 34$  ms the toroidal field is reducing and, combined with peaking of the current profile, this causes  $m=1$  activity to occur. This leads to the occurrence of sawteeth of period  $\sim 0.7$  ms from 37 ms, which results in a broadening of the pressure profile

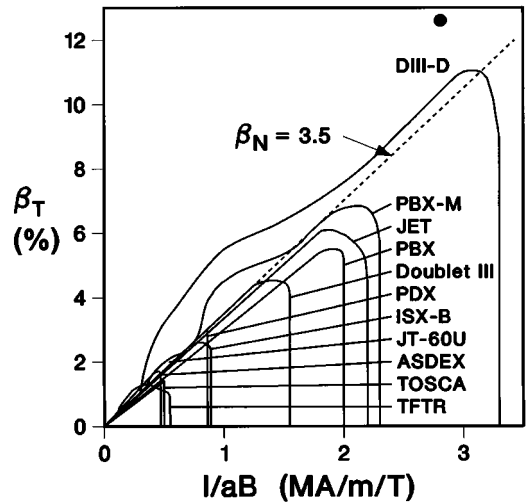


FIG. 6. Comparison of experimentally observed beta limits and Troyon scaling showing the operational envelopes for a number of tokamaks. Data compiled Sept. 1993; reproduced from Ref. 9.

as observed on the Thomson scattering and SXR diagnostics.

#### IV. BETA VALUES OBTAINED IN START

In his 1993 review Strait<sup>9</sup> compared the beta values obtained on world tokamaks in the  $\beta_T$  vs  $I/aB$  diagram shown in Fig. 6. The diagonal line indicates the Troyon limit  $\beta_{\max} = \beta_N / aB$  drawn for the limiting value  $\beta_N = 3.5$ . Each machine appears to reach (or slightly exceed) the  $\beta_N = 3.5$  limit, suggesting that the maximum beta achievable for each device is largely determined by the position of the right-hand boundary, which corresponds to a stability limit at field line edge  $q$ ,  $q_s = 2$ .<sup>9–12</sup> The DIII-D<sup>13</sup> tokamak has achieved the world's highest tokamak beta values to date, with the record average beta value of 12.6% which occurred at  $I/aB = 2.81$  in DIII-D shot 80108.

Tokamaks of larger aspect ratio than DIII-D (which had  $A \sim 2.9$  for the high-beta experiments) are further restricted in that the  $q_s \sim 2$  limit occurs at smaller values of  $I/aB$ . Conversely, as outlined in the Introduction, spherical tokamaks can operate at higher values of  $I/aB$  before meeting the  $q_s$  limit, even allowing for the predicted increase in this  $q$  limit as  $A$  reduces (see Sec. VI).

The START data shown in Fig. 7 supports this. Data from the H $\rightarrow$ H, H $\rightarrow$ D and D $\rightarrow$ D experiments are shown. In each case, the beam energy is  $\sim 30$  keV and the total power supplied is typically 400 kW, comparable to the Ohmic power of the plasma. It is seen that H $\rightarrow$ D operation (open circles) yielded slightly higher values of  $\beta$  than H $\rightarrow$ H (triangles) at each  $I/aB$ ; this may be associated with improved energy confinement in deuterium plasmas. The one-day D $\rightarrow$ D campaign, indicated by the filled circles in Fig. 7, achieved somewhat lower  $\beta$  values, but these results are very interesting in that modeling predicted low beam absorption due to the increased charge-exchange losses of beam ions expected with D $\rightarrow$ D operation in START. Also shown in Fig. 7 are the location of the low- $n$  and high- $n$  stability limits for 30868, predicted by the ERATO code. Operation with in-

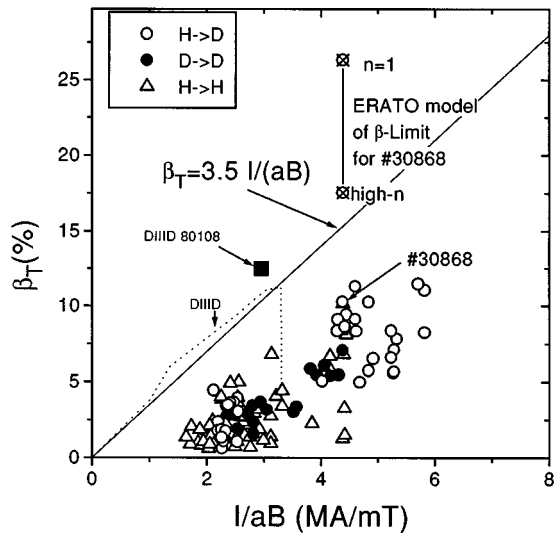


FIG. 7. Comparison of START data, with  $P_{NB} \sim P_{OH}$  showing the conventional Troyon scaling  $\beta_{max} = 3.5 I/aB$  (diagonal line). The limits of stability predicted by the ERATO code are shown for #30868.

creased NBI power for the same discharge parameters is expected to increase the beta up to these values.

The highest total beta value obtained for the present level of beam power ( $P_{NB} \sim P_{OH}$ ) is  $\beta_T \sim 11.8\%$  in #31832,

with  $\beta_N = 2.6$ ,  $\beta_O = 42\%$ . More peaked discharges have obtained central beta values up to 50%.<sup>7</sup>

## V. MHD BEHAVIOR DURING INJECTION

Low  $m, n$  mode activity seen during a typical injection experiment was described in Sec. III. This, together with the associated profile modification, becomes even more apparent when the toroidal field is substantially reduced in order to obtain high beta values. A reduction in the central electron pressure, accompanied by a flattening of the electron density profile and a decrease in the central ion temperature, is also seen. Analysis of SXR and Mirnov coil data shows that in different cases this MHD activity can be either an  $m/n = 1/1$  slow rotating mode, as in #30866 (Fig. 8) or coupled low- $n$  Mirnov activity with  $m/n = 2/1, 3/1$  and other harmonics. Very often sawtooth activity is seen following these low- $n$  fluctuations. High frequency “chirping” mode activity, similar to that reported on DIII-D,<sup>13</sup> is also observed. These modes are likely to be energetic particle modes associated with the fast ion pressure.

There are several possible explanations of the MHD and profile broadening under these conditions. First, that the reduction in toroidal field reduces  $q$ , exciting mode activity and eventually  $m/n = 1/1$  or sawtooth activity when  $q_0$  falls below unity, which then broadens the profile. Second, that the NBI deposition profile broadens in time as the plasma

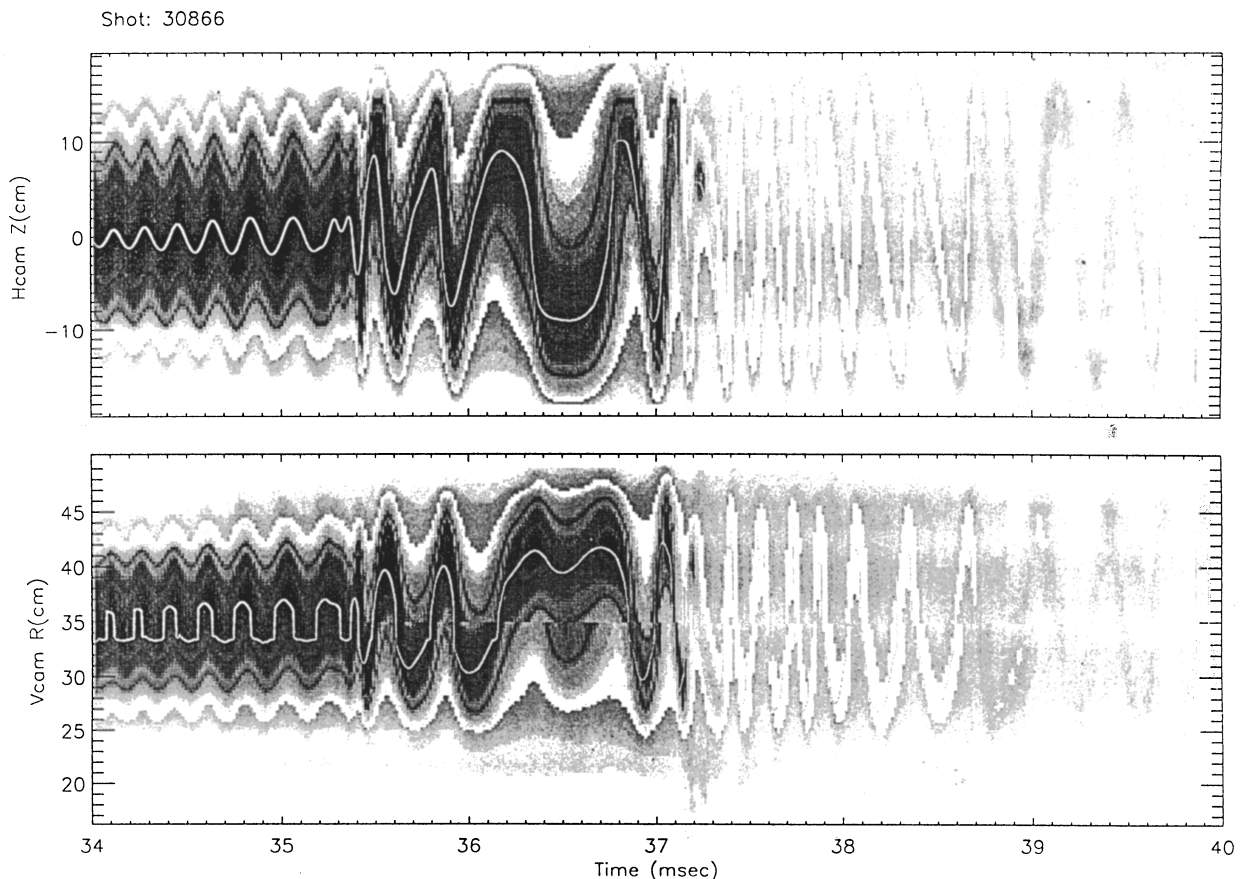
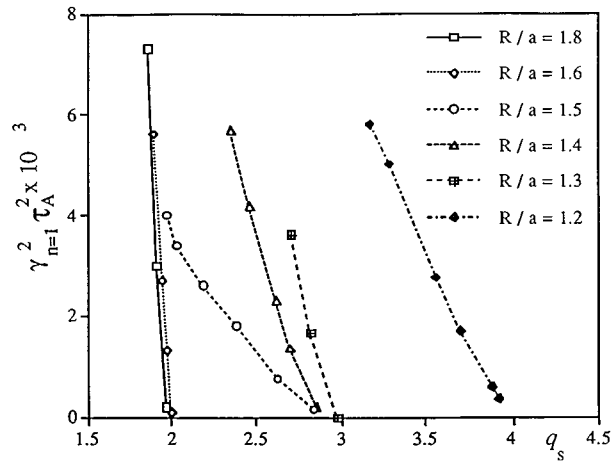
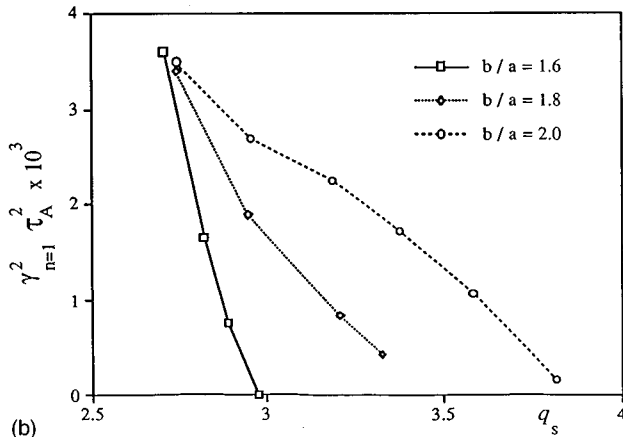


FIG. 8. SXR signals from horizontal (top) and vertical cameras showing a rotating  $m = 1$  mode which for this example slows and reverses direction at  $t \sim 36.5$  ms.



(a)



(b)

FIG. 9.  $n=1$  external kink growth rate ( $\beta=0$  model) for triangularity  $\delta=0.25$ , current profile  $\langle J_\phi \rangle \sim (1-\psi)$ ,  $q(0)=1.15$ , with remote wall, for (a) different  $R/a$  with elongation  $\kappa=1.6$ , (b) different  $\kappa$  at aspect ratio  $R/a=1.3$ .

density increases; leading in turn to broader pressure and current profiles which could excite  $m=2,3$  modes. A third possibility is that the MHD activity is driven directly by the increased pressure.

It is difficult at present to determine which combination of these effects is important in the START discharges reported here. It is not considered likely that the MHD is imposing a limit, because to date, each increase of NBI power has resulted in the attainment of higher  $\beta$  values and, as reported in the previous section, the theoretical (high- $n$  ballooning and  $n=1$  kink) limits should not be met until considerably higher  $\beta$  values are achieved. Application of increased beam power should soon resolve this question. Neoclassical tearing modes found to impose lower limits on beta in collisionless discharges<sup>14,15</sup> are not considered a problem for the high-density, relatively collisional plasmas in START.

## VI. THE $q$ -LIMIT

As described in Sec. III, typical START discharges with NBI heating evolve in the normal way, usually experiencing one or more internal reconnection events (IREs) as the cur-

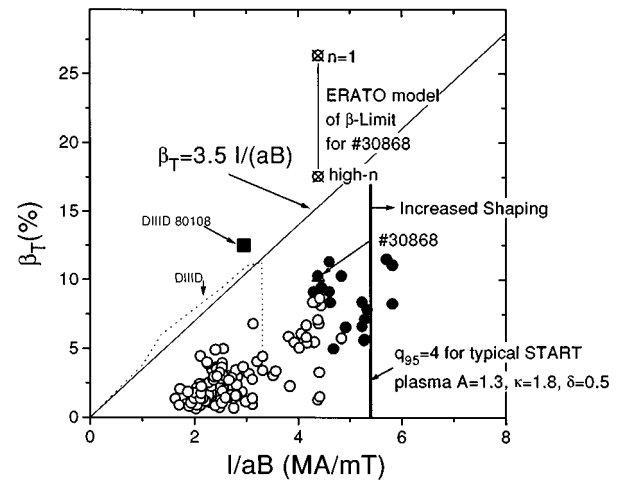


FIG. 10. START data, as in Fig. 7, here indicating (vertical line) the position of  $q_{95}=4$  for a typical START plasma ( $A=1.3$ ,  $\kappa=1.8$ ,  $\delta=0.5$ ). Discharges that terminated within 2 ms are here indicated by full symbols.

rent decays. Reduction of the toroidal field during the discharge is found to lead to large increases in beta as expected, together with MHD and profile changes as described in the previous section. The toroidal field can be reduced until a  $q$ -limit is met.

The results of kink mode stability studies using the ERATO code<sup>16</sup> are summarized in Fig. 9. These are for a pressureless model, and for a “natural divertor” (i.e., plasma limited on the center column) configuration, and suggest that as aspect ratio  $A$  reduces, the requirement  $q_s > 2$  applicable to conventional tokamaks becomes more restrictive in that  $q_s > 4$  may be required<sup>6</sup> for  $A \sim 1.2$ , although this is more than compensated by the increase in  $I/aB$  at low  $A$ . Increasing pressure does not change the picture significantly.<sup>3</sup>

The START beta data is replotted in Fig. 10, where the vertical line indicates the position of  $q_{95}=4$ , for a typical START DND plasma of  $A=1.3$ ,  $\kappa=1.8$ , triangularity  $\delta=0.5$ . It is seen that this boundary is consistent with the observed experimental results. The solid symbols in Fig. 10 indicate shots that terminated within 2 ms (approximately one confinement time) of the  $\beta$  measurement: see for example Fig. 4(a). These occur only at the high  $I/aB$ , low- $q$  limit of operations but for a range of  $\beta$  values so they appear to be associated with a low- $q$  limit rather than a beta limit. Previous low- $q$  operation, performed before the installation of the X-point coils, exhibited a milder sequence of IREs which did not terminate the plasma. This “disruption resilience” is also a feature of Current Drive Experiment-Upgrade (CDX-O) and MEDUSA operation.<sup>17,18</sup> A significant factor may be the use of double-null divertor (DND) discharges, produced by the X-point (divertor) coils shown in Fig. 1. These were installed in October 1995 and may influence the progress of an IRE in two different ways. Firstly, their very presence may cause severe interaction as the plasma increases in elongation, an important feature of the IRE in START.<sup>3</sup> Moreover, the X-point coils on START were only operated at low currents for this campaign, so that the X-point is close to the coil, as shown, for example, in Fig. 1. The simulations reported in Ref. 3 were carried out

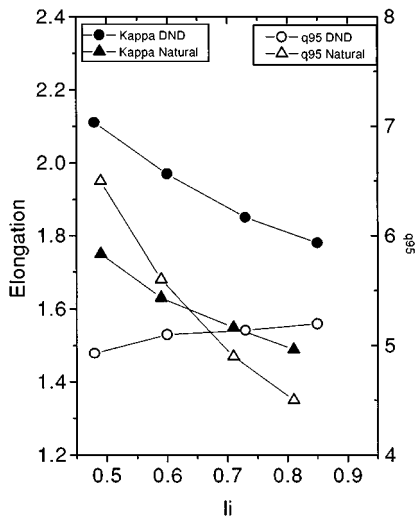


FIG. 11. Elongation  $\kappa$  versus internal inductance  $l_i$  for DND and limited plasma equilibria. Although elongation increases in both cases as  $l_i$  falls,  $q_{95}$  from TOPEOL exhibits quite different behavior, rising rapidly as  $l_i$  falls in “natural” limited plasmas, but reducing in DND plasmas.  $I_p$ ,  $R_o$ , and  $B_T$  held constant.

for limited plasmas, and it was found that plasma elongation associated with an IRE also acts to increase the value of  $q_{95}$ , which may stabilize low- $m$  instabilities. This feature, which is unique to low aspect ratio, is believed to play a key role in preventing an IRE leading to a major disruption at low  $A$  as discussed in the next section.

## VII. EFFECT OF AN IRE ON EDGE SAFETY FACTOR

The results described in Ref. 3 were applicable to naturally limited plasmas in START. A series of equilibrium code studies have been carried out to investigate key features of an IRE in DND plasmas. For simplicity, the plasma current is kept constant, and the plasma major radius is kept fixed by adjusting the vertical field. Plasma equilibria chosen are based on profiles typical of the high beta campaign. The internal inductance  $l_i$  is then varied by adjusting the pressure profile. For a naturally limited plasma in START, the dashed curve in Fig. 11 shows that the elongation increases markedly if  $l_i$  reduces, from 1.48 at  $l_i=0.8$  to 1.73 at  $l_i=0.5$ . However, the corresponding DND plasma has the plasma height effectively fixed by the ratio of X-point coil currents to plasma current; the elongation is already 1.8 at  $l_i=0.8$  and this rises to 2.07 at  $l_i=0.5$ , a smaller proportional increase than for the natural limited plasma. Moreover, the increase in elongation for the present DND plasmas is mainly achieved by reducing the width of the plasma rather than increasing its height, so that the aspect ratio increases, from 1.24 to 1.40 in the DND example of Fig. 11. This tends to reduce  $q_{95}$ . So in this typical example, the DND plasma experiences a *reduction* in  $q_{95}$  from 5.25 to 4.9, which could further destabilize the driving mode. In contrast, a corresponding naturally limited plasma of initially the same  $\beta$ ,  $l_i$ , and major and minor radii experiences an *increase* in  $q_{95}$  from 4.5 to 6.5 (Fig. 11) as  $l_i$  reduces, tending to stabilize the driving mode.

In an actual IRE, the total plasma current increases (typically by 10%–30%) and so the net effect on  $q_{95}$  in a low aspect ratio limiter plasma is usually a small increase; however, these results suggest a substantial reduction in  $q_{95}$  will occur due to an IRE in a DND plasma.

## VIII. FORWARD PROGRAM

Several improvements to START are being made during the October–November 1996 shutdown. The X-point and OH coils are being repositioned to provide slightly smaller plasmas and, moreover, remove the plasma from contact with the induction coil cases (Fig. 1), as this is presently a possible source of high- $Z$  contamination. Improved power supplies for the X-point coils will permit DND operation with X-points further removed from the coils, to investigate if the rapid terminations are then avoided. Single-null operation will also be investigated, as this should allow a more natural elongation of the plasma at an IRE. The power supplies are being enhanced to provide increased flux swing from the central solenoid, in order to obtain longer flat-top at high plasma current, and to provide increased vertical field necessary to contain the high-beta plasmas.

The beam energy will be raised to 40 keV from its present level of 30 keV, and it is expected that, with sufficient conditioning, the beam current can be raised from its present level of 60 A towards the 100 A formerly used at ORNL. In addition, installation of a getter pump in the neutral beam injector is planned and this should allow a doubling of injection power (due to a considerable increase in neutralization of the beam), even at the present levels of ion beam current and energy. This should, in conjunction with the other modifications, permit studies of energy confinement time under auxiliary heating, in addition to the main objective of exploring the Troyon limit.

## IX. SUMMARY AND CONCLUSIONS

The beta values measured on START are already comparable with the world’s highest tokamak beta reported on DIII-D. Moreover, START operation is not yet optimized and the auxiliary heating power, although high, is still comparable to  $P_{OH}$  in these high-density plasmas. The results reported here therefore represent a convincing demonstration of the high-beta capabilities of the spherical tokamak concept. Further development on START, both of beam power and of discharge optimization, is expected to extend considerably these results. Work will be carried forward on the MAST (Mega-Amp Spherical Tokamak) device<sup>19</sup> now under construction. MAST is a 1–2 MA machine, with ultrahigh vacuum, feedback controlled long pulse discharges, and with electron cyclotron resonant heating (ECRH) and NBI heating. Designed to exploit further the potential of the Spherical Tokamak and to extend the tokamak database, MAST is scheduled to obtain first plasma in 1998.

## ACKNOWLEDGMENTS

This work is presented on behalf of the START, NBI, and interpretation teams at UKAEA Fusion, Culham, with particular thanks to R. Akers, R. I. Buttery, P. G. Carolan, N.

J. Conway, G. F. Counsell, T. Edlington, M. Gryaznevich, T. C. Hender, I. Jenkins, S. Manhood, K. Morel, A. W. Morris, M. P. S. Nightingale, C. Ribeiro, C. Roach, D. C. Robinson, M. Valovic, M. J. Walsh, H. R. Wilson, O. J. Kwon (Taegu University, South Korea), R. Martin (UMIST, Manchester, UK), M. Mironov and V. Shevchenko (Ioffe Institute, St Petersburg, Russia), and M. Tournianski (Essex University). We wish to acknowledge the enthusiasm and practical assistance of ORNL personnel, in particular Y.-K. M. Peng, Jim Tsai, and R. Colchin, and thank CRPP Lausanne for use of the ERATO code, and T. Taylor and E. J. Strait of General Atomics for information on the DIII-D results.

This work is funded by the UK Department of Trade and Industry and Euratom. Shipment of the NBI equipment was funded by the U.S. Department of Energy.

<sup>1</sup>F. Troyon, R. Gruber, H. Saurenmann, S. Semenzato, and S. Succi, *Plasma Phys. Controlled Fusion* **26**, 209 (1984).

<sup>2</sup>A. Sykes, M. F. Turner, and S. Patel, *Proceeding of the 11th European Conference on Controlled Fusion and Plasma Physics*, 1983, Aachen (European Physical Society, Petit-Lancy, Switzerland, 1983), Vol. 2, p. 363.

<sup>3</sup>R. Akers, R. A. Bamford, M. K. Bevir, R. J. Buttery, A. Caloutsis, P. G. Carolan, N. J. Conway, M. Cox, G. F. Counsell, T. Edlington, C. G. Gimblett, M. Gryaznevich, T. C. Hender, I. Jenkins, O. J. Kwon, R. Martin, M. Mironov, K. Morel, A. W. Morris, M. P. S. Nightingale, M. R. O'Brien, Y.-K. M. Peng, S. Petrov, P. D. Phillips, C. Ribeiro, D. C. Robinson, S. E. Sharapov, A. Sykes, C. C. Tsai, M. Tournianski, M. Valovic, and M. J. Walsh, "Stability and additional heating properties of spherical tokamak plasmas on START," in *Proceedings of the 16th IAEA Conference*, Montreal, paper IAEA-CN-64/C2-1, 1996 (International Atomic Energy Agency, Vienna, in press).

<sup>4</sup>A. Sykes, E. del Bosco, R. J. Colchin, G. Cunningham, R. Duck, T. Edlington, D. H. J. Goodall, M. P. Gryaznevich, J. Holt, J. Hugill, J. Li, S. J. Manhood, B. J. Parham, D. C. Robinson, T. N. Todd, and M. F. Turner, *Nucl. Fusion* **32**, 694 (1992).

<sup>5</sup>A. Sykes, G. W. Crawford, G. Cunningham, N. A. Fawlk, D. H. J. Goodall, M. P. Gryaznevich, J. Hugill, I. Jenkins, R. Martin, C. Ribeiro, D. C. Robinson, R. T. C. Smith, T. N. Todd, M. J. Walsh, and B. J. Ward, "The START spherical tokamak," in *Proceedings of the 16th SOFE Conference*, Illinois, 1995 (Institute of Electrical and Electronics Engineers, New York, 1996), Vol. 2, p. 1442.

<sup>6</sup>D. C. Robinson, R. Buttery, I. Cook, M. Cox, M. Gryaznevich, T. C. Hender, P. Knight, A. W. Morris, M. R. O'Brien, C. Ribeiro, A. Sykes, T. N. Todd, M. Walsh, and H. R. Wilson, "The way forward for the spherical tokamak," *American Nuclear Society Topical Meeting*, June 1996 (American Nuclear Society, LaGrange Park, IL, in press).

<sup>7</sup>M. J. Walsh, R. Akers, R. Buttery, D. Codling, N. Conway, M. Gryaznev-

ich, T. Gunston, T. C. Hender, I. Jenkins, O. J. Kwon, R. Martin, M. Mironov, M. P. S. Nightingale, S. Petrov, C. Ribeiro, D. C. Robinson, R. T. C. Smith, A. Sykes, and S. E. V. Warder, "Record central beta produced by NBI in the START Spherical Tokamak," *Proceedings of the 21st EPS Conference*, Kiev, 1996 (European Physical Society, Petit-Lancy, in press).

<sup>8</sup>M. J. Walsh, R. J. Akers, R. A. Bamford, R. J. Buttery, P. G. Carolan, D. M. Codling, N. J. Conway, G. F. Counsell, M. Cox, J. Dowling, M. Gryaznevich, T. Gunston, I. Jenkins, R. Martin, M. Mironov, M. P. S. Nightingale, Y.-K. M. Peng, M. N. Price, C. Ribeiro, D. C. Robinson, M. Singleton, R. T. C. Smith, A. Sykes, J. Tsai, and S. E. V. Warder, "First results of neutral beam heating in START spherical tokamak plasmas," *Proceedings of the 21st EPS Conference*, Kiev, 1996 (European Physical Society, Petit-Lancy, in press).

<sup>9</sup>E. J. Strait, *Phys. Plasmas* **1**, 1415 (1994).

<sup>10</sup>DIII-D team, *Proceedings 13th IAEA Conference, Washington* (International Atomic Energy Agency, Vienna, 1991), p. 69.

<sup>11</sup>E. J. Strait, T. S. Taylor, A. D. Turnbull, J. R. Ferron, L. L. Lao, B. Rice, O. Sauter, S. J. Thompson and D. Wroblewski, *Proceedings of the 21st EPS*, Montpellier (European Physical Society, Petit-Lancy, 1994), Vol. I, p. 242.

<sup>12</sup>E. Lazarus, L. L. Lao, T. H. Osborne, T. S. Taylor, A. D. Turnbull, M. S. Chu, A. G. Kellman, E. J. Strait, J. R. Ferron, R. J. Groebner, W. W. Heidbrink, T. Carlstrom, F. J. Helton, C. L. Hsieh, S. Lippmann, D. Schis-sel, R. Snider, and D. Wroblewski, *Phys. Fluids B* **4**, 11 (1992).

<sup>13</sup>W. Heidbrink, *Plasma Phys. Controlled Fusion* **37**, 937 (1995), for general information on DIII-D, See J. L. Luxon and L. G. Davis, *Fusion Technol.* **8**, 441 (1985).

<sup>14</sup>J. W. Connor, R. O. Dendy, C. G. Gimblett, R. J. Hastie, P. Helander, T. C. Hender, K. G. McClements, J. B. Taylor, and H. R. Wilson, "Operational limits for advanced tokamaks," *Proceedings of the 16th IAEA Conference* Montreal, paper IAEA-CN-64/DP-3, 1996 (International Atomic Energy Agency, Vienna, in press).

<sup>15</sup>R. J. La Haye, J. D. Callen, M. S. Chu, S. Deshpande, T. A. Gianakon, C. C. Hegna, S. Jardin, L. L. Lao, J. Manickam, D. A. Monticello, A. D. Turnbull, and H. R. Wilson "Practical beta limit in ITER-shaped discharges in DIII-D and its increase by higher collisionality," in Ref. 14, paper IAEA-FI-CN-64/AP1-21.

<sup>16</sup>R. Gruber, *Computer Phys. Commun.* **21**, 323 (1981).

<sup>17</sup>M. Ono, D. Stutman, Y. S. Hwang, W. Choe, J. Menard, T. Jones, E. Lo, R. Armstrong, M. Finkenthal, V. Gusev, S. Jardin, R. Kaita, J. Manickam, T. Munsat, R. Nazikian, and Y. Petrov, "Investigation of the effect of resistive MHD modes on spherical torus performance in CDX-U," in Ref. 14, paper IAEA-CN-64/C2-2.

<sup>18</sup>G. D. Garstka, R. J. Fonck, and T. Intrator (private communication).

<sup>19</sup>A. C. Darke, M. Cox, J. R. Harbar, J. H. Hay, J. B. Hicks, J. W. Hill, D. Hurford, J. S. McKenzie, A. W. Morris, M. P. S. Nightingale, T. N. Todd, G. M. Voss, and J. R. Watkins, "The mega-amp spherical tokamak," in *Proceedings of the 17th SOFE Conference*, 1996 (Institute of Electrical and Electronics Engineers, New York, in press).